Modified Quantum and Phase Control of Series Resonant Converter

Woo H. KWON and Gyu H. CHO
Department of Electronic Engineering
Korea Advanced Institute of Science and Technology
P.O.Box 150, Chongryang, Seoul 130-650, Korea
FAX : (011)-822-960-2103

Abstract

New modified output voltage control scheme for the series resonant converter (SRC) is proposed. In this scheme, quantized output voltage is obtained by quantum duty control and one last unit voltage is continuously adjusted by phase angle control during a half resonant cycle period. Therefore the proposed control method offers a clue to get rid of the stepped discontinuity problem in the output voltage of quantum control without degrading the performance. Based on the steady state analysis, optimum quantum sequence having greatly reduced output voltage ripple is given.

In this paper new control method of quantum series resonant converter (QSRC) is proposed which is able to control the output voltage continously to reduce the output voltage ripple. In this scheme, quantized output voltage is obtained by the quantized duty control of ideal QSRC, while one quantized level voltage is continuously controlled by adjusting the phase angle during one quantum period(half resonant period). Therefore the proposed method of mixed quantum and phase angle control can adjust the output voltage of QSRC continuously having linear DC/DC characteristics like conventional PWM converters including all the other merits of resonant converters. However the output voltage ripple varies with switching sequence of QSRC in the quantum duty control method, thus the optimum quantum sequence (OQS) which is to minimize the output voltage ripple is suggested based on the steady state analysis.

I. INTRODUCTION

Recently, there has been an interest in the area of quantum resonant converter (QRC) [1, 2] which enables semiconductor switchings at true zero currents or true zero voltages. Such an operation shows very low switching losses at high frequency and allows the reduction of passive components. Therefore the QRC has many advantages such as small size, light weight, low component stress, high efficiency and low EMI. The QRC also operates at fixed resonant frequency over wide load range, which makes the determination of the optimal filter size easy in the output. However QRC has one critical disadvantage of discontinuous output voltage because it is controlled by the quantum numbers of the half cyle powering periods.

On the other side, the operation of resonant converters above and below resonance have been subjects of intensive researches because of their continuous control capability of output voltage. In this case, the switching frequency varies in a wide range having highly nonlinear DC characteristics and the operation at light load becomes difficult.

In order to control the output voltage and to reduce the switching stresses, quasi-resonant [3] and phase shifted resonant converters [4] are proposed. In the quasi-resonant converter, the output voltage is also controlled by varying the switching frequency in a wide range depending on the load condition. The latter uses two such converters in phase shifted manner to obtain constant frequency of operation. The main disadvantage of the phase shift control is the need for two separate resonant circuits having unbalanced voltages and currents. Efficiency also decreases at light load due to the circulating currents.

II. OPERATING MODES AND CONTROL METHOD OF QSRC

A. Ideal QSRC

The basic power circuit topology of the SRC is shown in Fig. 1. The SRC has four distinct operating modes [1]: the powering mode which increases the output voltage and the free resonant, regeneration and discontinuous modes which decrease the output voltage. Hence the output vlotage can be controlled by appropriate combinations of the powering mode and one of the other modes. In this paper, the regeneration and discontinuous modes are excluded from the discussion for higher input power factor and easy control. In other words only the powering and free resonant modes are considered.

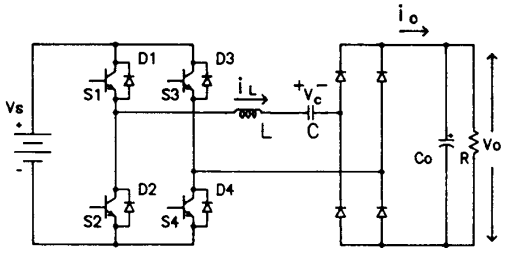

Fig. 1 Power circuit of QSRC.

0-7803-0090-4/91/0700-0498$01.00 ©1991IEEE

B. Operating Modes of Modified QSRC

The switch on/off control of QSRC always occurs in synchronization with the current zero crossing points. Therefore, the output voltage has quantized level.

In order to control the output voltage continuously, one quantized level voltage is continuously controlled by adjusting the phase angle during one quantum interval. In this case, the power circuit of modified QSRC is the same as the ideal QSRC, but it has five operating modes: powering, phase angle control, free resonant, regeneration and discontinous modes. The equivalent circuit for k-th quantum interval is shown in Fig. 2. As indicated in Fig. 2, $M(k)$ is control variable (+1, 0, -1: $M(k)$=1 for powering mode, -1 for regenerative mode and 0 for free resonant mode) for the regulation of output voltage in the continuous conduction mode (CCM) at M-QSRC where V_s^* is effective input source voltage. The angle θ is either 0 or π for ideal QSRC [i.e., $M_k = 1, \theta = 0$ for powering mode , $\theta = \pi$ for free resonant mode] while θ varies in between 0 and π at $M_k = 1$ for the phase angle control method.

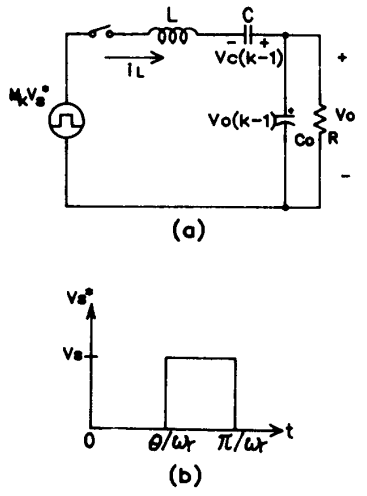

Fig. 2 Modified QSRC (a) generalized equivalent circuit (b) control input waveform.

Throughout the paper, it is assumed that the quality factor Q and the output capacitor C_o are sufficiently large so that the converter always operates in the CCM and the output voltage change during a quantum period is negligible. Then control input V_s^* is given by

$$V_s^* = V_s \{ U_s(t-\theta/\omega_r) - U_s(t-\pi/\omega_r)\}. \tag{1}$$

Therefore, from the equivalent circuit, the tank circuit current $i_L(k)$ is given by

$$i_L(k) = \frac{V_c(k-1)-V_o(k-1)}{Z}\sin(\omega_r t)U_s(t) + \frac{M_k V_s}{Z}\sin(\omega_r t-\theta)U_s(t-\frac{\theta}{\omega_r})$$

$$= \begin{cases} \dfrac{V_c(k-1)-V_o(k-1)}{Z}\sin(\omega_r t) & \text{at } 0 < t < \dfrac{\theta}{\omega_r} \\ \sqrt{P^2+R^2}\,\sin(\omega_r t-\theta_p) & \text{at } \dfrac{\theta}{\omega_r} < t < \pi \end{cases} \tag{2}$$

where,

$$P = \frac{V_c(k-1)-V_o(k-1)+M_k V_s\cos\theta}{Z},$$

$$R = \frac{M_k V_s \sin\theta}{Z},$$

$$\theta_p = \tan^{-1}\left\{\frac{R}{P}\right\},$$

$$\omega_r = 1/\sqrt{(LC)}, \qquad Z = \sqrt{(L/C)}.$$

The angle θ_p of equation (2) is the shift angle which is generated in this modified phase angle control. θ_p is a function of V_c, V_o and V_s but in practice V_c is larger than V_s and θ_p nearly approaches to zero. The tank capacitor peak voltage $V_c(k)$ can be evaluated as follows :

$$V_c(k) = \frac{1}{C}\int_0^{T/2} i(t)dt - V_c(k-1)$$

$$= \frac{1}{CZ}\int_0^{T/2} (V_c(k-1) - V_o(k-1))\sin(\omega_r t)U_s(t)\,dt + \frac{1}{CZ}\int_0^{T/2} M_k V_s \{\sin(\omega_r t-\theta_p)U_s(t-\theta/\omega_r))\,dt - V_c(k-1) \tag{3}$$

where,

$$T = 2\pi\sqrt{LC}.$$

From eq. (3) we can obtain the discrete state equation for $V_c(k)$ as

$$V_c(k) = V_c(k-1) + 2[\lambda M_k V_s - V_o(k-1)] \tag{4}$$

where,

$$\lambda = \cos^2(\theta/2).$$

In equation (4), λ is the effective output voltage which is given by a function the phase angle θ. The output voltage of QSRC for the modified phase angle control can be evaluated as

$$V_o(k) = \frac{1}{C_o}\int_0^{T/2} i(t)dt + V_o(k-1) - \frac{1}{C_o R}\int_0^{T/2} V_o(k-1)\,dt. \tag{5}$$

Therefore the discrete state equation of the output voltage is determined by the control angle θ and can be written as

$$V_o(k) = \gamma V_c(k-1) + (1-\gamma-\gamma^*) V_o(k-1) + \gamma M_k \lambda V_s \tag{6}$$

where,

$$\gamma = 2(C/C_o) \text{ and } \gamma^* = \pi/2\,(Z/R)\,\gamma.$$

C. Average Value of Integral Cycle Mode Control[2]

The waveforms of the QSRC that is controlled under the condition of the quantum period n, powering mode m and the phase control angle θ, is shown in Fig. 3.

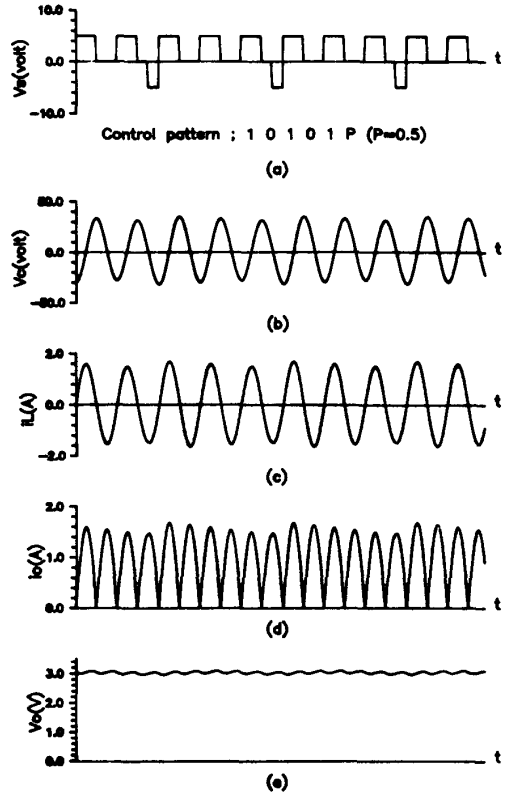

Fig. 3 Waveforms of QSRC at control sequence $\{M_k|k=6:1\ 0\ 1\ 0\ 1\ P\ (\theta=\pi/2)\}$ for L=80μH, C=0.2μF, Co=30μF, R=3Ω: (a) input switching volatge (b) capacitor voltage (c) inductor current (d) output current (e) output voltage.

The steady state tank capacitor voltages from (k+1)-th half resonant period to (k+n)-th half resonant period are given by

$$\begin{aligned} V_c(k+1) &= V_c(k) + 2\,(A_1M_1V_s - V_o(k)) \\ V_c(k+2) &= V_c(k+1) + 2\,(A_2M_2V_s - V_o(k+1)) \\ &\vdots \\ V_c(k+n) &= V_c(k+n-1) + 2\,(A_nM_nV_s - V_o(k+n-1)) \\ &= V_c(k)\ . \end{aligned} \tag{7}$$

From eq. (7), summation of the tank capacitor voltage is given by

$$\sum_{i=0}^{n-1} V_c(k+i) = \sum_{i=0}^{n-1} V_c(k+i) + 2\left\{ \sum_{i=1}^{n} A_iM_iV_s - \sum_{i=0}^{n-1} V_o(k+i) \right\}. \tag{8}$$

Therefore, generally, the average value of the steady state output voltage $V_{o\text{-}av}$ is given by from eq. (8) as

$$\begin{aligned} V_{o\text{-}av} &= \sum_{i=0}^{n-1} V_o(k+i)/n \\ &= \sum_{i=1}^{n} A_iM_iV_s/n \\ &= \left[\sum_{i=1}^{n} M_i + \cos^2\left(\frac{\theta}{2}\right) \right] \left(\frac{V_s}{n}\right) \\ &= \frac{V_s}{n}\left[m + \cos^2\left(\frac{\theta}{2}\right) \right]. \end{aligned} \tag{9}$$

In a similar manner, we can obtain the average tank capacitor voltage $V_{c\text{-}av}$ and the peak average inductor current $I_{L\text{-}av}$. From eq. (6), the average tank capacitor voltage is given by

$$\begin{aligned} V_{c\text{-}av} &= \sum_{i=0}^{n-1} V_c(k+i)/n \\ &= \frac{\pi}{2}\,\frac{Z}{R}\,V_{o\text{-}av}\ . \end{aligned} \tag{10}$$

And the peak average inductor current is given by

$$I_{L\text{-}av} = \frac{V_{c\text{-}av}}{Z}\ . \tag{11}$$

Therefore the average output current is given by

$$\begin{aligned} I_{o\text{-}av} &= \left| \frac{2}{\pi} I_{L\text{-}av} \right| \\ &= \left| \frac{V_{o\text{-}av}}{Z} \right|. \end{aligned} \tag{12}$$

The output average voltage which is given by eq. (9) consists of discontinuous and continuous voltages. The discontinuous output voltage is determined by the powering mode number m of QSRC and the continuous voltage is controlled from 0 to V_s/n (one quantum voltage step) by the phase control angle θ. Therefore the output voltage is continuously controllable over all voltage range by the variation of m and θ for a given n. Even though the control characteristics of phase control angle θ is given by $\cos^2(\theta/2)$, the output voltage can be linearly controlled through appropriate transformation of θ.

Fig. 4 represents the characteristics of the output voltage versus the phase control angle θ of this modified QSRC at n=5, m=3. It is shown that the theoretical value matches closely to that of simulation result.

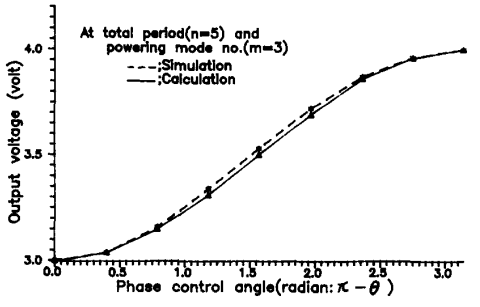

Fig. 4 Output voltage vs. phase angle θ control.

D. Analysis of Ouput Voltage Ripple

The output voltage ripple in the modified QSRC is generated from the two different currents : steady state average and instantaneous output currents. Thus they can be considered as two harmonic sources and the corresponding output ripples. They are defined as sinusoidal ripple and envelope ripple respectively. The sinusoidal ripple is induced from the difference between the rectified sinusoidal current and its average and this ripple is always generated but small. On the other hand, the envelope ripple that is generated from the variations of the envelope of rectified sinusoidal harmonic current is large and varies with switching sequence of QSRC in the quantum duty control method. This ripple is theoretically calculated from the difference between the rectified fluctuation current and the average rectified current. Hence it can be calculated as follows:

$$\Delta V_{o\text{-}rip2} = \frac{2}{\pi C_o \omega_r} \left[\mathrm{Max}\left\{ \int_0^{\theta} \Delta I_o(x)dx \right\} - \mathrm{Min}\left\{ \int_0^{\theta} \Delta I_o(x)dx \right\} \right] \quad (13)$$

$$\text{for } 0 \le \theta \le n\pi$$

where,

$$\Delta I_o(x) = \left[\frac{I_o(k+1) - I_o(k)}{\pi} (x - k\pi) + I_o(k) \right] - I_{o\text{-}av}$$

$$\text{for } k\pi \le x \le (k+1)\pi,\ k = 0,1,2,\ldots,n-1 .$$

$I_o(k)$, $I_{o\text{-}av}$ are determined from equations (2) and (12) when the quantum sequence $\{M_k | M_k : k=1,2,\ldots,n\}$ is given. Therefore the equation (13) can be solved numerically. Table 1 illustrates the normalized output voltage ripples for different powering modes m with optimized quantum sequences(OQS).

Table 1 Output voltage ripple of quantum and phase control (phase control angle $\theta=\pi/2$).

		Simple duty control		Optimum quantum sequence control	
n	m	sequence	ripple(%)	sequence	ripple(%)
3	1	1 0 P	0.797	1 P 0	0.610
	2	1 1 P	0.660	1 1 P	0.660
4	1	1 0 0 P	1.111	1 0 P 0	0.818
	2	1 1 0 P	0.917	1 0 1 P	0.734
	3	1 1 1 P	0.695	1 1 1 P	0.695
5	1	1 0 0 0 P	1.547	1 0 P 0 0	0.936
	2	1 1 0 0 P	1.320	1 0 1 P 0	0.620
	3	1 1 1 0 P	1.026	1 1 P 1 0	0.723
	4	1 1 1 1 P	0.729	1 1 1 1 P	0.729
6	1	1 0 0 0 0 P	2.100	1 0 0 P 0 0	1.224
	2	1 1 0 0 0 P	1.853	1 0 1 0 P 0	0.958
	3	1 1 1 0 0 P	1.505	1 0 1 0 1 P	0.858
	4	1 1 1 1 0 P	1.131	1 1 0 1 1 P	0.820
	5	1 1 1 1 1 P	0.763	1 1 1 1 1 P	0.763

n : Total period.
m : Powering mode number.
P : Phase control angle.

(phase control angle = $\pi/2$)

		Simple duty control		Optimum quantum sequence control	
n	m	sequence	ripple(%)	sequence	ripple(%)
7	1	1 0 0 0 0 0 P	2.765	1 0 0 P 0 0 0	1.523
	2	1 1 0 0 0 0 P	2.509	1 0 0 1 0 P 0	0.890
	3	1 1 1 0 0 0 P	2.116	1 0 1 0 1 P 0	0.625
	4	1 1 1 1 0 0 P	1.682	1 1 0 1 P 1 0	0.764
	5	1 1 1 1 1 0 P	1.234	1 1 1 P 1 1 0	0.821
	6	1 1 1 1 1 1 P	0.796	1 1 1 1 1 1 P	0.796
8	1	1 0 0 0 0 0 0 P	3.540	1 0 0 0 P 0 0 0	1.863
	2	1 1 0 0 0 0 0 P	2.854	1 0 0 1 0 P 0 0	1.014
	3	1 1 1 0 0 0 0 P	2.854	1 0 1 0 P 1 0 0	1.040
	4	1 1 1 1 0 0 0 P	2.364	1 1 0 P 1 0 1 0	0.942
	5	1 1 1 1 1 0 0 P	1.854	1 1 0 1 1 P 1 0	0.761
	6	1 1 1 1 1 1 0 P	1.336	1 1 1 0 1 1 1 P	0.911
	7	1 1 1 1 1 1 1 P	0.830	1 1 1 1 1 1 1 P	0.830

It is shown that the OQS's are obtained when the powering modes are evenly distributed whereas the worst quantum sequences are obtained when they are concentrated.

III. SIMULATION AND EXPERIMENTAL RESULTS

Previous results need to be tested since the proposed model includes several assumptions and approximations. This can be accomplished by comparing the analytical results with the time domain simulation results. To obtain the exact solution, the following state equations are written for the original circuit of Fig. 1 and 2 :

$$\frac{d}{dt}\begin{bmatrix} i_L(t) \\ V_c(t) \\ V_o(t) \end{bmatrix} = \begin{bmatrix} 0 & -1/L & -s_2(t)/L \\ 1/C & 0 & 0 \\ s_2(t)/C_o & 0 & -1/C_oR \end{bmatrix} \begin{bmatrix} i_L(t) \\ V_c(t) \\ V_o(t) \end{bmatrix} + \begin{bmatrix} s_1(t)/L \\ 0 \\ 0 \end{bmatrix} V_s \quad (14)$$

where,

$$s_1(t) = \begin{cases} \mathrm{sgn}(i_L(t)) & \text{, powering mode} \\ 0 & \text{, free resonant mode} \\ \mathrm{sgn}(i_L(t))*[U(t-\theta/\omega_r)-U(t-\pi/\omega_r)] & \text{, phase angle control mode} \end{cases}$$

and

$$s_2(t) = \mathrm{sgn}(i_L(t))$$

$$\mathrm{sgn}(i_L(t)) = \begin{cases} 1, & i_L(t) \ge 0 \\ -1, & i_L(t) < 0 . \end{cases}$$

The switching function $s_1(t)$ is externally controllable by the duty control quantum sequence $\{M_k\}$, however, $s_2(t)$ which represents the diode rectification status is internally controlled by the inductor current. For simulation and experiments, the following circuit parameters are used :

L= 80μH, C=0.2μF, Co=150μF, R=3Ω .

Fig. 5(a) shows the gate signals for ouput control when duty control quantum sequence M_k is given as $\{M_k|k=8$: 1011011P, P=0.5$\}$ and (b) and (c) show the tank capacitor voltage and tank inductor currnt, respectively, and (d) shows the output voltage waveform.

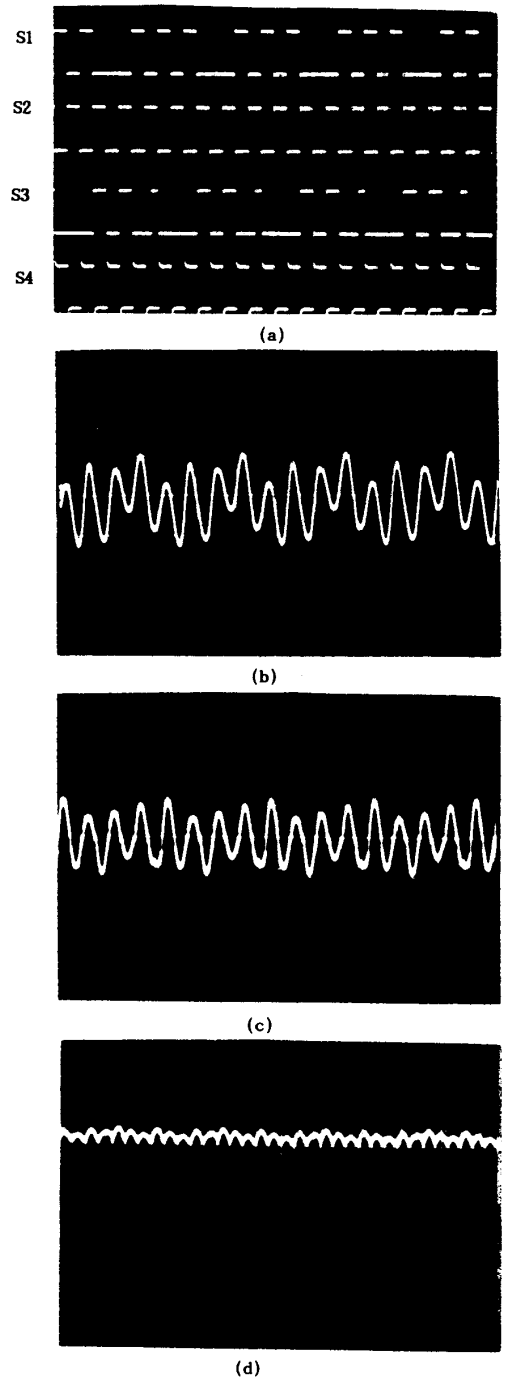

Fig. 5 Waveforms of (a) gate signals, (b) capacitor voltage, (c) inductor current and (d) output voltage .

Fig. 6 shows dc transfer function of simulation and measured data with the theoretical values. The transfer function characteristic of simulation and theoretical results coincided well. The small difference is due to the increasing effect of the output voltage caused by switching overlap intervals. But the measured data show lower gain than the theoretical ones, which is mainly thought to be due to the conduction loss such as FET, inductor and capacitor series resistances and voltage drop across the rectifier diode. The measured values match well with the theoretical values when the conduction losses are taken into account.[2]

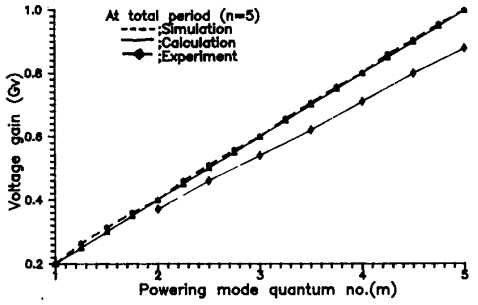

Fig. 6 Output voltage gain(Gv) vs. powering mode no.(m) of time and phase control method.

The waveforms of the transient responses are shown in Fig. 7 where the duty control quantum sequences are (a) $\{M_k|k=6$: 111000$\}$, (b) $\{M_k|k=6$: 101010$\}$ and (c) $\{M_k|k=6$: 10101P, P=0.5$\}$, respectively. The results show that the control methods do not influence important effect to the transient response but do affect the output voltage ripple.

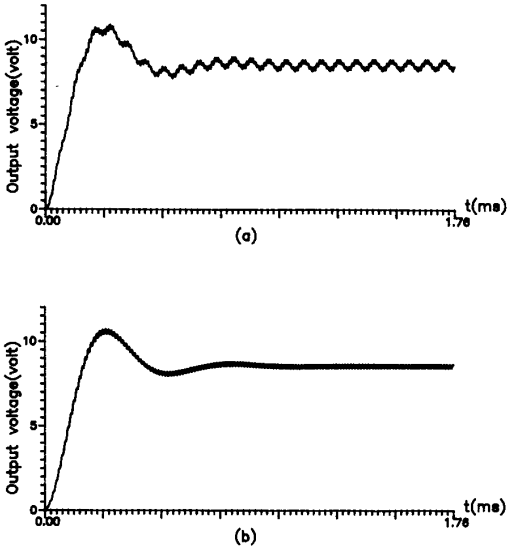

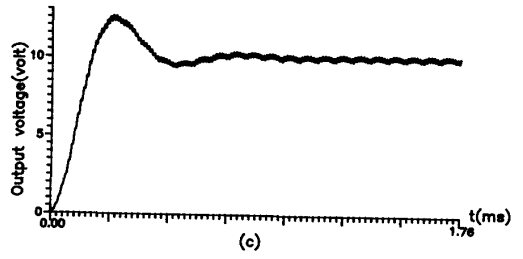

Fig. 7 Transient response characteristics of QSRC : (a) {M_k:111000} (b) {M_k:101010} (c) {M_k:10101P, P=0.5} for L=80μH, C=0.2μF, Co=30μF and R=3Ω .

Fig. 8 shows the output voltage ripple as a function of voltage gain at n=5. This result shows superiority of the OQS to the worst case. In simple duty control case, a large difference between the calculated and the simulated value appeares at low voltage gain. It is due to the discontinuous conduction mode (DCM).

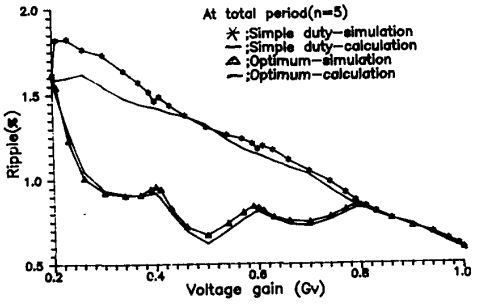

Fig. 8 Ripple vs output voltage gain for L=80μH, C=0.2μF Co=150μF and R=3Ω.

IV. CONCLUSION

This paper describes a new modified control method of QSRC for continuous control of output voltage. In this scheme a quantized output is obtained by the quantum duty control. In addition, one quantum voltage is continuously controlled by varying the phase angle during one quantum period (half resonant time interval). Therefore almost linear DC/DC characteristic is obtained with low switching loss and low EMI noise as well. Finally based on the steady state analysis, the optimum quantum sequence for minimizing the output voltage ripple is determined.

References

[1] G.B. Joung, C.T. Rim, and G.H. Cho, "Modeling of quantum series resonant converters - controlled by integral cycle mode," *IEEE - IAS conf. rec.*, 1988, pp.821-826.

[2] G.B. Joung, C.T. Rim, and G.H. Cho, "Integral cycle mode control of the series resonant converter," *IEEE Trans. on power electronics* 1989, PE-4, pp.83-91.

[3] K.H. Liu, R. Oruganti, and F.C.Y. Lee, "Quasi - resonant converter - topologies and characteristics," *IEEE Trans. on power electronics*, 1987, PE-1, No.1, pp.62-71.

[4] I.J. Pitel, "Phase - modulated resonant power conversion techniques for high - frequency link inverter," *IEEE Trans. Ind. Appl., IA-22*, No.69, pp.1044-1051.